J. Sci. I. R. Iran

Vol.9 No.2
Spring 1998

FISSION FRAGMENT ANGULAR ANISOTROPIES AND INERTIA PARAMETERS

A.N. Behkami and P. Nazarzadeh

Department of Physics, Shiraz University, Shiraz, 71454, Islamic Republic of Iran

Abstract

An analysis of selected fission fragment angular distributions from helium-ion induced fission is made using an exact theoretical expression. Theoretical anisotropies obtained with the transition state model are compared with their corresponding values deduced from the statistical scission model. The nuclear moment of inertia extracted from the model calculations are compared with their estimated values from a microscopic theory, which includes the nuclear pairing interaction [1]. Single particle levels of Nilsson *et al.* are utilized. It is found that the value of the statistical parameter, K_o^2(K_o^2=J_{eff} T/h^2) is very sensitive to the energy gap parameter, Δ. The reduction of energy gap results in an increase in the moment of inertia. The effect of pairing interaction on the inertia parameters is illustrated and discussed.

Introduction

There is considerable evidence that the statistical transition model (TSM) provides a good representation of experimental fission fragment angular distributions at low spin values and moderate excitation energies. The fundamental assumption of this model is that the spin projection, K, on the nuclear symmetry axis remains unchanged during the fission process. For heavy reaction systems, where the angular momentum and excitation energy are large, fission fragment angular distributions are analyzed with the statistical scission model (SSM). Versions of this model have been published by Rossner *et al.* [2] and Bond [3]. Although the formal equation in the two models is of the same structure, variances in the distributions of angular momentum projections on the fission direction are established at very different stages of the fission process in the two models. The properties of transition state complex were studied by various authors [4-6]. Nuclear moments of inertia were extracted from the measured fission fragment anisotropies, Huizenga *et al.* [7]. A sharp decrease in J_{sph}/J_{eff} with Z^2/A at relatively low spin has been observed calling for shell and/or pairing effects [8].

In the present work, we have developed a special computer code to deduce the statistical parameter K_0^2(K_0^2= J_{eff} T/h^2), from experimental angular anisotropies using the exact theoretical expressions. The K_0^2 values have also been evaluated by employing the microscopic theory of interacting fermions using the single particle levels of the Nilsson model. Our microscopic calculations of the inertia parameters are in satisfactory agreement with experiment, especially at lower spin values and moderate excitation energies. In Section 2, we review the basic theoretical framework. Variances of the spin distribution obtained from model calculations based on both the transition state and the statistical scission models are presented in Section

Keywords: Fragment angular distributions in (α, f) reactions

3.a. In Section 3.b, the dependence of K_0^2 on excitation energy and nuclear deformation will be presented and the resulting inertia parameters, obtained from microscopic theory, will be compared with their corresponding experimental values.

2.a. Formalism of Transition State Model at Moderate Excitation Energies

The excited levels in the transition nucleus are described by statistical theory. The K-distributions of these levels are predicted by Halpern *et al.* [9] to be Gaussian

$$F(K) \propto \exp\left(\frac{-K^2}{2K_0^2}\right) \qquad (1)$$

and the variance of the distributions is

$$K_0^2 = \frac{J_{eff}\,T}{h^2} \qquad (2)$$

The effective moment of inertia is $J_{eff} = J_{II}J_{\perp}/(J_{II} + J_{\perp})$, where $J_{\perp}$ and J_{II} are nuclear moment of inertia about an axis perpendicular and parallel to symmetry axis and T is the temperature of the nucleus in the transition state.

Assuming that the fragments separate along the symmetry axis and that K is a good quantum number during the fission process, then the fragment angular distribution from a state with quantum numbers K and M (projection of total spin I along the space fixed axis) is given by [10]

$$W^I_{M,K}(\theta) = [(2I+1)/4\pi/]\, d^I_{M,K}(\theta)\,|^2 \qquad (3)$$

The normalized $d^I_{M,K}(\theta)$ functions are defined by [11]

$$d^I_{M,K}(\theta) = [(I+M)!\,(I-M)!\,(I+K)!\,(I-K)!]^{1/2}$$

$$\sum_x \frac{(-1)^x (\sin(\theta/2))^{K-M+2x} (\cos(\theta/2))^{2I-K+M-2x}}{(I-K-X)!\,(I+M-X)!\,(X+K-M)!\,X!} \qquad (4)$$

Where the sum is over X= 0,1,2,... and contains all terms in which no negative value appears in the denominator of the sum for any one of the quantities in parentheses.

If the target and projectile spins are zero and no particle emission from the initial compound nucleus occurs before fission (i.e. M = 0), then the overall angular distribution for a fixed energy E is given by Griffin [12]

$$W(\theta) \propto \sum_{I=0}^{\infty} (2I+1)\,T_I \sum_{K=-I}^{I} [(2I+1)\,|d^I_{M=0,K}(\theta)|^2 \exp\left(\frac{-K^2}{2K_0^2}\right) \Big/ \sum_{K=-I}^{I} \exp\left(\frac{-K^2}{2K_0^2}\right)] \qquad (5)$$

Where the transmission coefficients are written as T_l, since $l = I$ when M = 0.

Equation (5) is an exact theoretical expression for computation of fission fragment angular distribution when both the target and projectile spins are zero. If the target and projectile spins are included, an exact expression for the fission fragment angular distribution is [11, 12]

$$W(\theta) \propto \sum_{I=0}^{\infty} \sum_{M=-j_{max}}^{+j_{max}} [\sum_{l=0}^{\infty} \sum_{j=|I-s|}^{I+s} \sum_{\mu=-l}^{l} \frac{((2l+1)\,T_l\,|C_{M,0,M}^{j,\mu,l}|^2\,|C_{\mu,M-\mu,M}^{I_0,s,j}|^2)]}{\sum_{l=0}^{\infty} (2l+1)\,T_l}$$

$$\sum_{K=-I}^{I} [(2I+1)\,|d_{M,K^1}(\theta)|^2 \exp\left(\frac{-K^2}{2K_0^2}\right) \Big/ \sum_{K=-I}^{I} \exp\left(\frac{-K^2}{2K_0^2}\right)] \qquad (6)$$

The quantities I_0, s and j are the target spin, projectile spin and channel spin, respectively. The channel spin j is defined by the relation $j = I_0 \oplus s$. The total angular momentum I is given by the sum of the channel spin and orbital angular momentum: $I = j \oplus l$. The projection of Io on the space-fixed axis is given by μ, whereas the projection of j (and I) on this axis is M.

The use of Equations (5) or (6) requires the evaluation of many $d_{M,K^1}(\theta)$ functions and the Clebsch-Gordan coefficients, hence these equations have rarely been used for data analysis. In the present paper, we have developed a special computer code to run these more cumbersome theoretical expressions and thereby deduce the statistical variance K_0^2. We have found quite different values of K_0^2 as compared to the values from the approximate expression [13-15].

2.b. Formalism of the Statistical Scission Model

According to the statistical scission model, the relative cross-section, $W(\theta)$, for fission fragments to be emitted in the direction $\hat{n}$ forming angle θ with the beam axis, when the target projectile spins are zero, is given by Huizenga *et al.* [16]

$$W(\theta) \propto$$

$$\sum_{I_{min}}^{I_{max}} (2I+1)\, T_I \frac{\sum_{m=-I}^{I} [(2I+1)/2]\, |D^{I}_{M=0,m}(\theta)|^2 \exp(-m^2/2S_0^2)}{\sum_{m=-I}^{I} \exp(-m^2/2S_0^2)} \qquad (7)$$

Here again the distribution of spin projection m (the projection of total angular momentum I along $\hat{n}$) is taken to be a Gaussian with variance S_0^2, where S_0^2 for spherical fission fragments is given by either of the following equations [2]

$$S_0^2 = \begin{cases} 2\sigma^2 \{[2\sigma^2 + (\mu Rc^2 T/\hbar^2)]/(\mu Rc^2 T/\hbar^2)\}, \\ (2J_{sph} T/\hbar^2)\,[(2J_{sph} + \mu Rc^2)/\mu Rc^2] \end{cases} \qquad (8)$$

Where $\sigma^2 = J_{sph}\, T/\hbar^2 = \frac{2}{5} MR^2 T/\hbar^2$

The quantities J_{sph}, T,M and R, are the moment of inertia, nuclear temperature, mass and radius of one of the symmetric fission fragments. Rc is the distance between centers of fragments at scission configuration and is equal to $Rc = 1.225\,(A1^{1/3} + A2^{1/3})\,(c/a)^{2/3}$ (A1 and A2 are mass numbers of fission fragments). For a scission configuration of two unattached deformed fragments, the variance So^2 is given by either of two equations [2]

$$S_0^2 = \begin{cases} 2\sigma_{II}^2 \{[2\sigma_I^2 + (T\mu Rc/\hbar^2)]/[(T\mu Rc^2/\hbar^2) + 2\sigma_I^2 - 2\sigma_{II}^2\}, \\ [2J_{II} T/\hbar^2]\,[(2J_I + \mu Rc^2)/(\mu Rc^2 + 2J_I - 2J_{II})] \end{cases} \qquad (9)$$

Where $\sigma_{\parallel}^2$, $\sigma_{\perp}^2$, $J_{\parallel}$ and $J_{\perp}$ are spin cut-off parameters and moments of inertia of a single fission fragment rotating about an axis parallel and perpendicular to the symmetry axis, respectively. The primary fission fragments are assumed to have spheroidal shapes with the principal one-half axes of magnitude in terms of their ratio c/a namely [16]

$$c = r_0 A^{1/3} (c/a)^{2/3} \quad \text{and} \quad a = r_0 A^{1/3} (c/a)^{-1/3} \qquad (10)$$

Where A is the mass number of each fission fragment. The formula (7) is similar to the corresponding equation in the transition state model. However, as seen from Equations (8) and (9), the variance S_0^2 is calculated in a completely different way. The total intrinsic excitation energy in the two fission fragments at scission is given by

$$E = E_{cm} + Q - E_k - E_{def} - E_{rot} \qquad (11)$$

Where Q represents the difference in energy between the entrance channel nuclei and the ground state of the two fission fragments. $E_k + E_{def}$ is the sum of the kinetic and deformation energies at the instant of scission and E_{rot} is the rotational energy of the scission configuration. The kinetic energy is estimated by use of the expression

$$E_k\,(\text{MeV}) = 0.107 \frac{Z^2}{A^{1/3}} + 22 \qquad (12)$$

Where Z and A are the charge and mass number of the composite system. The rotational energy E_{rot} of the system at scission configuration for spin I and projection m on the scission axis is

$$E_{rot} = \frac{[(I+1/2)^2 - m^2]\,\hbar^2}{2\mu Rc^2 + 4J_{\perp}} \qquad (13)$$

μ is the reduced mass of the fission fragments. The temperature of each fission fragment was assumed to be given by

$$T = [(E/2)/LDP]^{1/2} \qquad (14)$$

The variances of the spin distribution can also be estimated with a microscopic theory of interacting fermions using a realistic set of single particle levels. For deformed fission fragments with axial symmetry, the single particle states are from the motion of a nucleon in the deformed average potential. They are characterized by the projection Ω of the angular momentum on the nuclear symmetry axis.

Employing the microscopic theory with nuclear pairing, the spin cut-off parameter $\sigma^2(E)$ is defined by [2,17]

$$\sigma_{II}^2(E) = J_{II} T/\hbar^2 = \frac{1}{2}\{\sum \Omega_{pi}^2 \operatorname{sech}^2(\tfrac{1}{2}\beta E_{pi}) + \sum \Omega^2_{ni} \operatorname{sech}^2 (\tfrac{1}{2}\beta E_{ni})\} \qquad (15)$$

Where $\beta = \frac{1}{T}$ (T is the nuclear temperature), E_{pi} is the proton quasi particle energy and E_{ni} is the neutron quasi particle energy. The quasi particle energies E_i are related to the single particle energies ε_i by $E_i = [(\varepsilon_i - \lambda)^2 + \Delta^2]^{1/2}$ where λ is the chemical potential and Δ is the ground state gap parameter. The quantity J_{II} is the moment of inertia about an axis parallel to the symmetry axis. The spin cut-off parameter σ_{II}^2 (E) is determined by the properties of the intrinsic state. Hence Equation (15) is a definition of the moment of inertia.

In so far as the neutron-proton superfluids are independent, the values of the thermodynamic functions are the sum of those for neutrons and protons. For example, the intrinsic excitation energy corresponding to a given temperature is

$$E_{int} = E^{p}_{int} + E^{n}_{int} \qquad (16)$$

Since the interaction between the neutron and proton is neglected, the values of the moment of inertia are the sum of the proton and neutron moments of inertia.

$$J = J_p + J_n \qquad (17)$$

The temperature dependence of J is investigated by examining the data on angular distribution of fission fragments. Such angular distributions depend on the statistical variance K_0^2 discussed in Section 2.a. This quantity is

$$K_0^2 = J_{eff}\, T/\hbar^2 = \left(\frac{T}{\sigma l^2 \hbar^2} - \frac{1}{J_l}\right)^{-1} T/\hbar^2 \qquad (18)$$

The dependence of K_0^2 upon excitation energy is therefore a good test of the persistence of superconducting effects to finite excitation energies. The dependence of K_0^2 versus the excitation energy for some typical cases of helium-induced fission reactions has been tested and the results will be given in the next section.

3.a. Results and Discussion

Several fission reactions are chosen to deduce the statistical variance, K_0^2 by fitting experimental fission fragment angular distributions with exact theoretical expressions which do and do not include the target and projectile spins. Angular distributions have been studied for fragments in the fission of ^{197}Au, ^{209}Bi, ^{233}U, ^{234}U, ^{235}U and ^{238}U by 42.8 MeV helium-ions. Optical-model transmission coefficients are used in all calculations and the α-particle transmission coefficients, Huizenga and Igo [18], are kept fixed for the calculations with different equations. The experimental anisotropy W(170)/W(90) for ^{238}U (He, f) reaction with 42.8 MeV is 1.52 taken from Gindler *et al.* [13]. The curve in Figure 1 illustrates the theoretical dependence of anisotropy of K_0^2 extracted from Equation (5), which assumes that both the target and projectile spins are zero. The curve in Figure 2 illustrates the theoretical dependence of anisotropy on K_0^2 for ^{209}Bi(He, f) reaction deduced from Equation (6), which includes the target and projectile spins. The fission fragment angular anisotropies together with the variances K_0^2, obtained from the listed anisotropies using the exact expressions, are given in Table I.

Examination of the K_0^2 given in Table I reveals that our K_0^2 values are in some cases smaller than their previously reported values. For example, the experimental anisotropy for ^{209}Bi(He, f) reaction is 2.12. The results of our exact theoretical calculation with spin of target and projectile included is 46.5 as compared to its reported value of 56, which is about 17% too small. This demonstrates the error introduced by neglecting the target and projectile spins. The measured fission fragment angular distributions at 42.8 MeV helium-induced fission of ^{197}Au and ^{209}Bi, taken from Chaudhry *et al.* [19], are fitted using the "best fit"

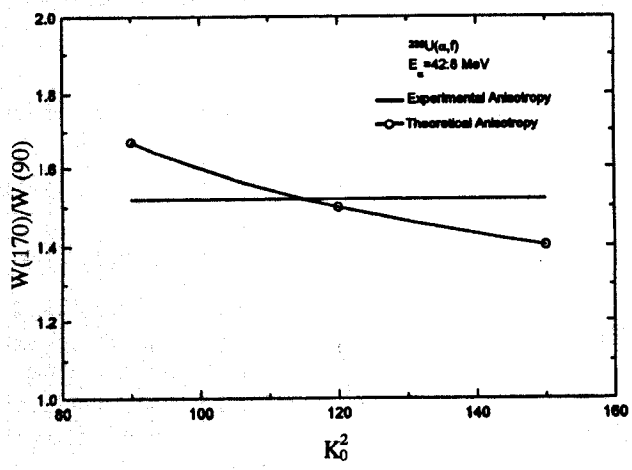

Figure 1. Anisotropy, W(170) / W(90), of fission fragments for ^{238}U(He,f) reaction with 42.8 MeV α-particles. The theoretical curve is calculated with Equation (5).

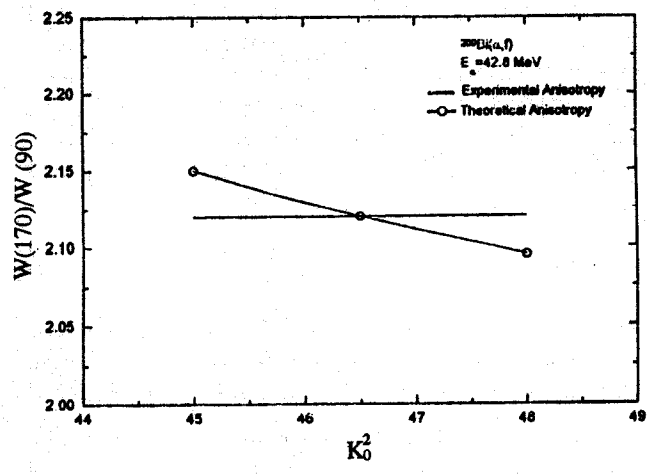

Figure 2. Anisotropy, W(170) / W(90), of fission fragments for ^{209}Bi(He, f) reaction with 42.8 MeV α-particles. The theoretical curve is calculated with Equation (6).

Table I. Anisotropies, K_0^2 and S_0^2 values determined from the exact theoretical fit to the data at 42.8 MeV helium ions

Target	$\frac{W(170)}{W(90)}$	K_0^2 [b]	K_0^2 [c]	S_0^2 [d]	S_0^2 [e]
^{197}Au	2.47	39	37.5	33.1	46.2
^{209}Bi	2.12	56	46.5	45.5	52.7
^{233}U	1.38	151	151.5	135	150
^{234}U	1.42	131	138	133	135.4
^{235}U	1.40	149	146	129	152.6
^{238}U	1.52	108	116.3	101	111

a) Anisotropy measurement taken from [13]

b) K_0^2 calculated from [13]

c) K_0^2 values obtained from the present work

d) Best fit values of S_0^2 with l_f= 20h

e) Theoretical values of S_0^2

values of K_0^2 from Table I; the results are displayed in Figure 3.

Variance S_0^2 has been evaluated by fitting the listed experimental fission fragment angular distributions using Equation (7) assuming l_f = 20h. Our best fit values are given in Table I. It is seen that in some cases the deduced values of S_0^2 are close to the values of K_0^2 calculated from the TSM model.

The variances S_0^2 have also been calculated, assuming spheroidal fragments at the scission configuration. These theoretical values of S_0^2 are computed using Equation (9) by assuming r_0 = 1.225 fm, a = A/8 and E_{def} = 10 MeV.

Our theoretical values of S_0^2 for deformed fragments are considerably smaller than their corresponding experimental values for uranium reactions. In order to bring the predicted values into agreement with the experimental variances, the level density parameter "a" would need to be increased from A/8 up to A/20. The results are shown in the last column of Table I.

We conclude that the variances K_0^2 produced by the TSM model for the 42.8 MeV helium-ion reactions give generally a good agreement relative to the SSM model. This reestablished the applicability of this model for systems with well-defined deformation and lower spin values at moderate energies.

Variances K_0^2 determined from the listed angular anisotropies at 42.8 MeV helium-ion induced fission are

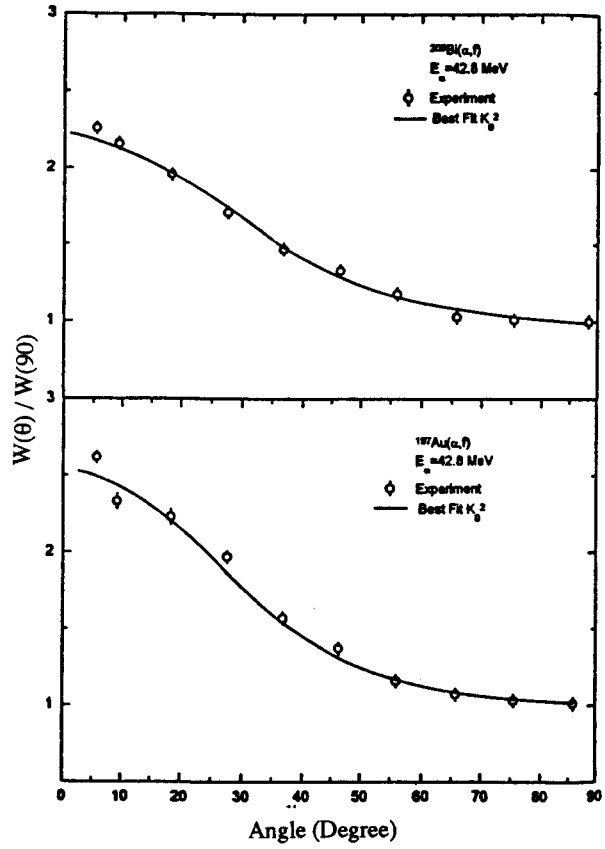

Figure 3. The angular distributions of fragments in the helium-ion induced fission of ^{197}Au and ^{209}Bi. The experimental data are given by open circles, and the solid curve shows the "best fit" K_0^2 calculated angular distributions.

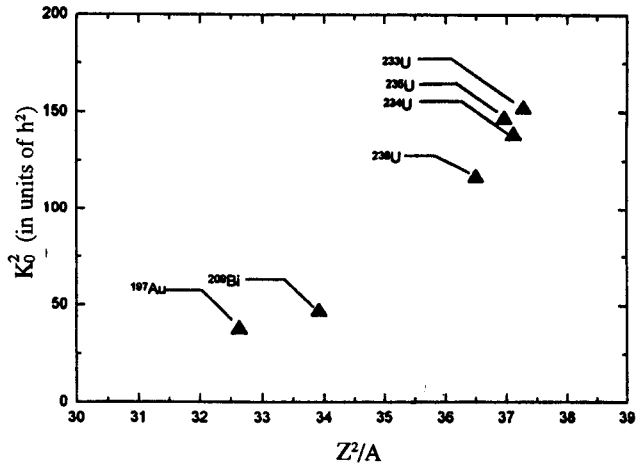

Figure 4. Values K_0^2 as a function of Z^2/A of the fissioning nucleus. The calculated variances are labelled according to the target nucleus.

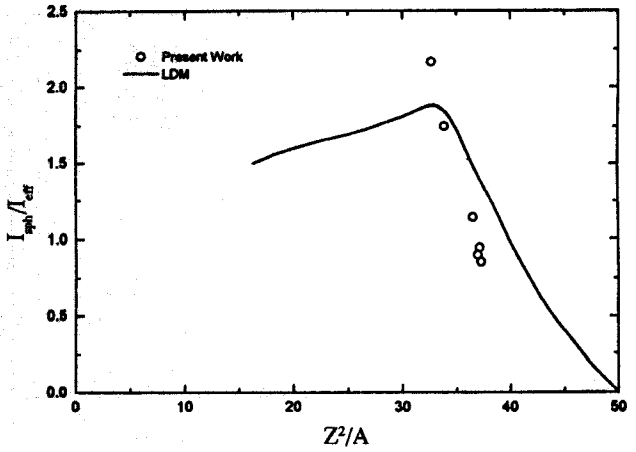

Figure 5. Comparison of the experimental values of J_{sph}/J_{eff}, determined from helium-ion induced reactions with the liquid drop model. Solid line curve represents the theoretical nonrotating (LDM) model values of J_{sph}/J_{eff} as a function of Z^2/A.

plotted in Figure 4 as a function of Z^2/A of the fissioning nucleus. It is seen from Figure 4 that the K_0^2 values tend to increase as the parameter Z^2/A of the compound nucleus increases. This is related to an increase in J_{eff} with Z^2/A. We have converted our "best fit" values of K_0^2 to values of J_{sph}/J_{eff} using Equation (2) by utilizing the appropriate nuclear temperature T. We have estimated the temperature for first and second chance fission. In Figure 5 we show results only for the assumption of first chance fission.

It is clear from Figure 5 that there is a distinct increase in J_{sph}/J_{eff} with decreasing Z^2/A. This is the effect observed by Simmons *et al.* [20], confirmed by others [21] and discussed in connection with dependence of K_0^2 on the excitation energy above fission barrier. The proposed explanation involves pairing energy and/or shell effects which will be discussed next.

3.b. Inertia Parameters

For determination of fission fragment anisotropies in the superconducting model, the most important parameter to be calculated is $J_{\parallel}T/\hbar^2$. This quantity is directly related to the average of K^2 over the particle spectrum and is given by the spin cut-off parameter, $\sigma^2_{\parallel}(E) = J_{\parallel}T/\hbar^2$.

The microscopic theory is used to compute $\sigma^2\parallel(E)$ by way of Equation (15). Values of $\sigma^2_{\perp}(E)$ are calculated with the rigid body moment of inertia for shape corresponding to deformation $\delta = 0.65$, although this assumption leads to an upper limit of $\sigma^2_{\perp}$ for small spin. K_0^2 values are calculated as a function of excitation energies for the case of helium-induced fission of ^{238}U nucleus. The energies and spins of the single particle levels were calculated with a program and parameters of Nilsson *et al.* [22]. The values of the gap parameters $\Delta_n = 1.23$ MeV and $\Delta p = 1.35$ MeV used in the present calculations were obtained from the newest mass table of G. Audi *et al.* [23]. Temperature dependence of the gap parameters for ^{242}Pu fissioning nucleus is shown in Figure 6.

In Figure 7, the moment of inertia for ^{242}Pu is plotted as a function of nuclear temperature. Intrinsic excitation energy (a) and entropy (b) are plotted in Figure 8 as a function of temperature.

Figure 9 shows experimental values of K_0^2 versus the excitation energy for ^{242}Pu together with theoretical curves calculated from the superconducting model for the shapes corresponding to $\delta = 0.37$ and $\delta = 0.65$. It is seen that the agreement between the calculation for the shape corresponding to $\delta = 0.65$ and the experiment is very

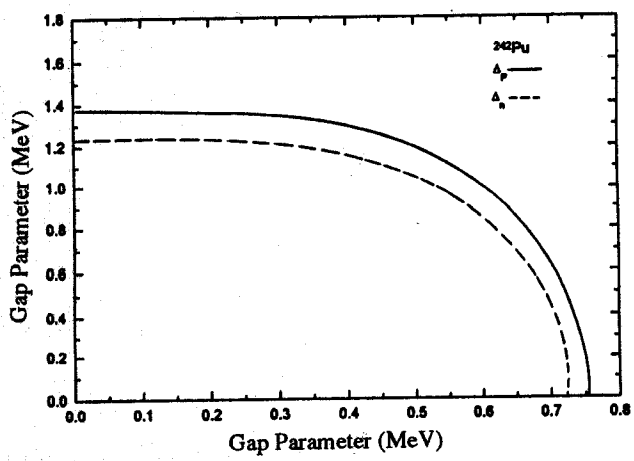

Figure 6. Temperature dependence of the neutron and proton energy gap parameters for ^{242}Pu nucleus

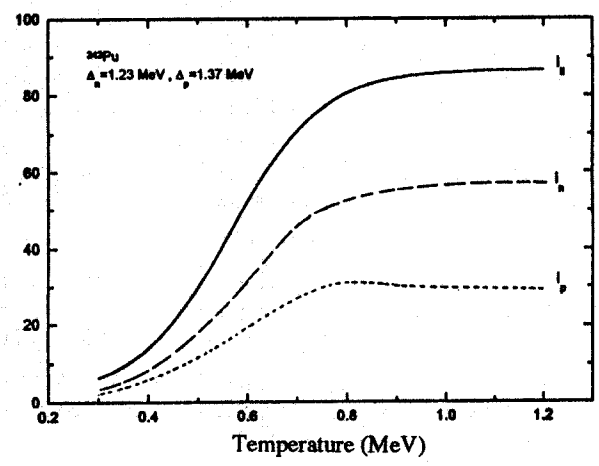

Figure 7. Temperature dependence of moments of inertia for ^{242}Pu nucleus

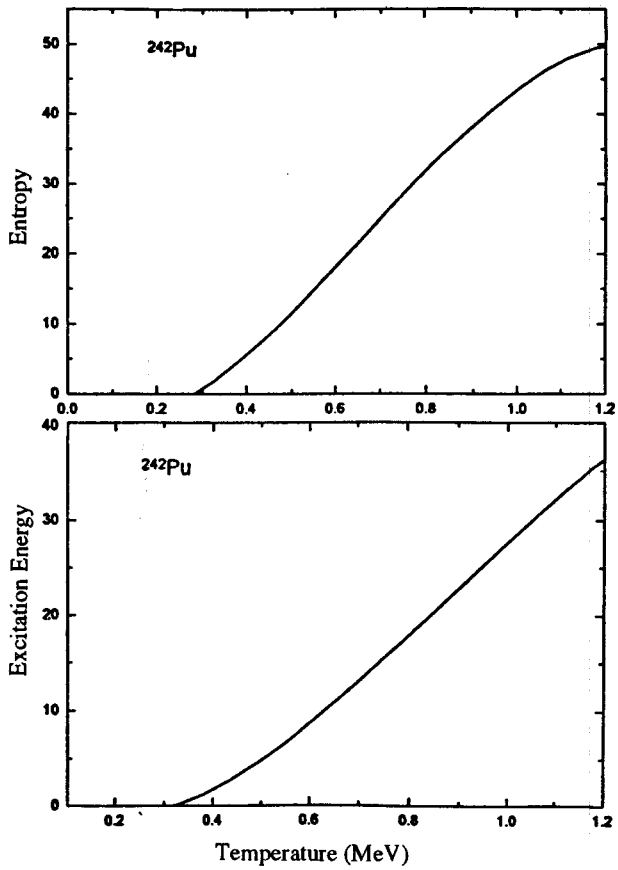

Figure 8. (a) Intrinsic excitation energy (b) entropy is plotted as a function of temperature for ^{242}Pu nucleus

good. The results from the LDM model are also plotted for comparison.

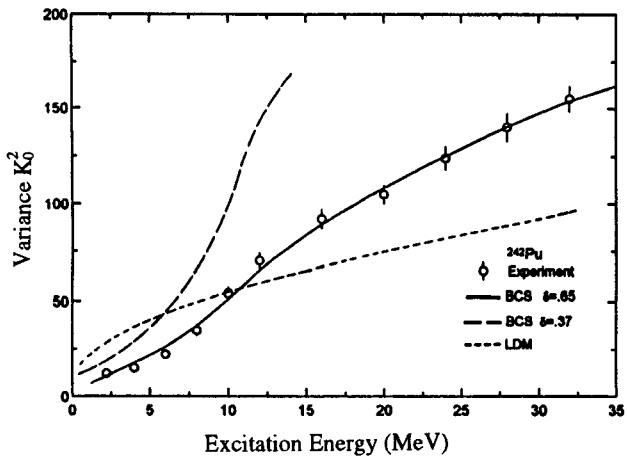

Figure 9. Variation of K_0^2 with the excitation energy of the nucleus ^{242}Pu. The experimental points are taken from [21]. The calculated values of K_0^2 corresponding to the barrier I ($\delta = 0.37$) and barrier II ($\delta = 0.65$) are shown by dashed and solid lines respectively.

References

1. Bardeen, J., Cooper, L.N. and Schrieffer, J.R. *Phys. Rev.*, **106**, 162, (1957).
2. Rossner, H., Huizenga, J.R. and Schroder, W.U. *Ibid.*, **C33**, (2), 560, (1985).
3. Bond, P.D. *Phys. Rev. Lett.*, **52**, 414, (1984).
4. Vandenboch, R. and Huizenga, J.R. *Nuclear fission.* Academic, New York, (1973).
5. Rossner, H. *et al. Phys. Rev.*, **C27**, 2666, (1981).
6. Ramamurthy, V.S. and Kapoor, S.S. *Phys. Lett.*, **54**, 178, (1985).
7. Huizenga, J.R., *et al. Phys. Rev.*, **177**, (4), 1826, (1969).
8. Vaz, L.C. and Alexander, J.M. *Phys. Report*, **97**, 1, (1983).
9. Halpern, I. *Ann. Rev. Nucl. Sci.*, **9**, 245, (1959).
10. Huizenga, J.R., Behkami, A.N., Meadows J.W. and Klema, E.D. *Phys. Rev.*, **174**, (4), 1539, (1968).
11. Huizenga, J.R., Moretto, L.G. and Behkami, A.N. *Ibid.*, **177**, (4), 1826, (1969).
12. Griffin, J.J. *Ibid.*, **B354**, 139, (1965).
13. Gindler, J. *et al. Nucl. Phys.*, **A145**, 337, (1970).
14. Tsang, M.B. *et al. Phys. Rev.*, **C28**, 747, (1983).
15. Prakash, M. *et al. Phys. Rev. Lett.*, **52**, 990, (1984).
16. Huizenga, J.R., Rossner, H.H. and Schroder, W.U. *J. Phys. Soc. JPN.*, **54**, 257, (1985).
17. Huizenga, J.R. *et al. Nucl. Phys.*, **A123**, 589, (1974).
18. Huizenga, J.R. and Igo, J. *Ibid.*, **29**, 462, (1962).
19. Chaudhry, R. *et al. Phys. Rev.*, **126**, 220, (1962).
20. Simmons, J.E. and Hofman, H. *Nucl. Phys.*, **A394**, 477, (1983).
21. Sano, M. and Wakai, M. *Progress of Theoretical Physics*, **48**, (1), 160, (1972).
22. Nilsson, S.G. *et al. Nucl. Phys.*, **A131**, 1, (1969).
23. Audi, G. and Wapstra, A.H. *Ibid.*, **A566**, 1, (1993).